Egyptian Journal of Chemistry

http://ejchem.journals.ekb.eg/

TRANSITION METAL COMPLEXES INCORPORATING SYMMETRIC tetra dentate Schiff base ligand: Synthesis, characterization, biological activities, DFT and molecular docking studies

Mohamed T. Radwan [1], Walaa H. Mahmoud [1], Mohamed A.F. ElMosallamy [2] and Ahmed A. El-Sherif [1]

[1] Department of Chemistry, Faculty of Science, Cairo University, Egypt

[2] Department of Chemistry, Faculty of Science, Zagazig University, Egypt

Abstract

Cr(III), Fe(II), Ni(II), Co(II), and Cu(II) complexes of a symmetric Schiff base ligand (L), N'-1-(2-(p-tolyl) hydrazono) propan-2-ylidene)-2-1-(2-(p-tolyl)hydrazono) propan-2 ylidene) hydrazine-1-carbothiohydrazide have been synthesized. Elemental analysis, UV-Visible, FT-IR, mass spectra, magnetic susceptibility, and conductometric techniques were used to characterise the ligand and its metal complexes. Gram-positive bacteria (Staphylococcus aureus, Staphylococcus faecalis, and Bacillus subtilis), Gram-negative bacteria (Neisseria gonorrhoeae, Pseudomonas aeruginosa, and Escherichia coli), and fungi were used to assess the antibacterial activity of the presented compounds (Candida alibicans). The synthesized complexes displayed potential antibacterial activity when evaluated by the in vitro approach against various bacterial and fungal strains. Comparing all of the studied species, Co(II) complex exhibits the highest activity versus all tested organisms. Based on the DFT level, structural characteristics and MEP of the synthesized compounds were computed and correlated with the experimental results. To determine the most favoured mode of interaction, molecular docking studies with a few chosen protein structures have been carried out using the DFT-optimized structures of the Schiff base and its Co(II) complex.

Keywords: Schiff base; spectra Molecular docking; DFT; Antimicrobial activity.

1. Introduction

Utilizing organic ligands with hetero atoms as coordination sites allows coordination chemistry to develop a wide range of intriguing and practical combinations. Furthermore, because of their powerful chelating potential to create mono-, di-, or multinuclear complexes, ligands with more than one heterodonor atom have drawn attention from all over the world in coordination chemistry [1, 2].A major contribution to the synthesis of metal-ligand bonds is also contributed by the lone pair of

*Corresponding author e-mail: aelsherif@sci.cu.edu.eg (Prof. Dr. Ahmed El-Sherif)

Received date 2023-01-10e; revised date 2023-04-13; accepted date 2023-05-25
DOI: 10.21608/EJCHEM.2023.186292.7436

electrons that are available on heteroatoms. Due to their extraordinary capacity for building complexes and extensive use as spectrometric and gravimetric reagents in analytical chemistry, Schiff base ligands with N, O, and S donor atoms have drawn a lot of attention over the years. Additionally, it has been claimed that administering these chemicals as metal complexes increases their action [1–9].The significance of transition metal complexes with a Schiff base ligand is mostly attributable to the wide range of industries they have found use in, including catalysis [10–16], chemosensors [17–18], luminous materials [19–20], energy materials [21–22], and biological sectors [23]. Particularly, complexes of metal ions with octahedral coordination preferences (such as Cu(II), Co(II), and Cr(III)) show significant physicochemical characteristics as well as biological activity [24]. These forms of substances are utilized for metal analyses as well as for telecommunications, optical computing, storage, and information processing device applications [25–32].are investigating Schiff bases with various functional groups adjacent to the condensation sites and their complexes with some metal ions from the first transition series as part of ou we are continuous interest in coordination chemistry [14, 15]. Different physicochemical methods of characterization were used. It was documented that this Schiff base's metal complexes have biological activity. The DFT-based B3LYP approach and the LANL2DZ basis set were used to thoroughly optimize the Schiff base ligand and its Co(II) complex. The study of charge distribution and quantum chemical parameters was conducted using MEP. In order to determine the most preferred binding type and, as a result, to justify the antimicrobial activity's mechanism, Schiff base docking with diverse proteins has been concentrated on. The prediction of drug-likeness and toxicity of synthetic molecules is made possible by the burgeoning field of docking [10–23].

2.Materials and methods

1.1. Experimental

2.1.1. Chemicals and reagents

In this study, high-purity chemicals were used. 1-(2-(p-tolyl)hydrazono)propan-2-one, hydrazinecarbothiohydrazide, $CrCl_3.6H_2O$, $FeSO_4.7H_2O$, $CoCl_2.6H_2O$, $NiCl_2.6H_2O$, and $CuCl_2.2H_2O$ were purscahsed from Merck. The organic solvents including ethyl alcohol (95%), acetone, DMSO (Dimethyl sulfoxide), and dimethylformamide (DMF) were provided by Sigma Chemical Co. in St. Louis, Missouri, USA. All preparations are typically performed using de-ionized water.

2.1.2. Solutions

Metal complexes of $1x10^{-3}$ M were dissolved in dimethylformamide in precisely weighed amounts to prepare stock solutions. By diluting the previously prepared stock solutions, solutions of the Schiff base ligand and its metal complexes ($1x10^{-5}$ M) were prepared for evaluating their UV-Vis spectra.

2.1.3. Instrumentation

The MS-5988 GS-MS Hewlett-Packard equipment was used to record mass spectra using the EI method at 70 eV. Using a Jenway 4010 conductivity meter, the molar conductivities of 10^{-3} M solutions of the solid complexes in DMF were determined. The CHNS-932 (LECO) Vario Elemental Analyzer was used to do microanalyses of carbon, hydrogen, nitrogen, and sulfur. The metals were analyzed after the solid complexes were dissolved in concentrated HNO_3, neutralizing the diluted aqueous solutions, and then quantified using the ICP(inductive coupled plasma) spectrometer Teledyne Leeman. Perkin-Elmer 1650 spectrometer was used to provide the Ft-IR spectrums of complexes in KBr pellets that captured in a range of 4000-400 cm^{-1}. Shimadzu 3101pc spectrophotometer was used to provide the electronic spectra of complexes at room temperature as DMSO-*d6* solutions. A 300 MHz Varian-Oxford Mercury was used to provide ^1H NMR spectra as a solution in DMSO-*d6* at room temperature and using TMS as an internal standard. The antimicrobial activities were studied on different organisms. All the pervious analyses were conducted at Microanalytical Center, Cairo University, Egypt.

1.2. Procedures

1.2.1. Synthesis of the Schiff base ligand [L]

The suggested approach was used to synthesize a novel Schiff base ligand. In order to do this, hydrazinecarbothiohydrazide (1 mmol, 0.107 g) and 1-(2-(p-tolyl)hydrazono)propan-2-one (2 mmol, 0.704 g) were condensed in hot 100% ethanol (60 °C). Thereafter, 4 hours of reflux were applied to the reaction mixture. Then, a pure Schiff base with a 93% yield was obtained from the DMF-ethanol mixture by evaporation, filtering out, and recrystallizing an orange solid chemical. The structure of the Schiff base ligand as well as its general formation reaction are shown in Scheme (1).

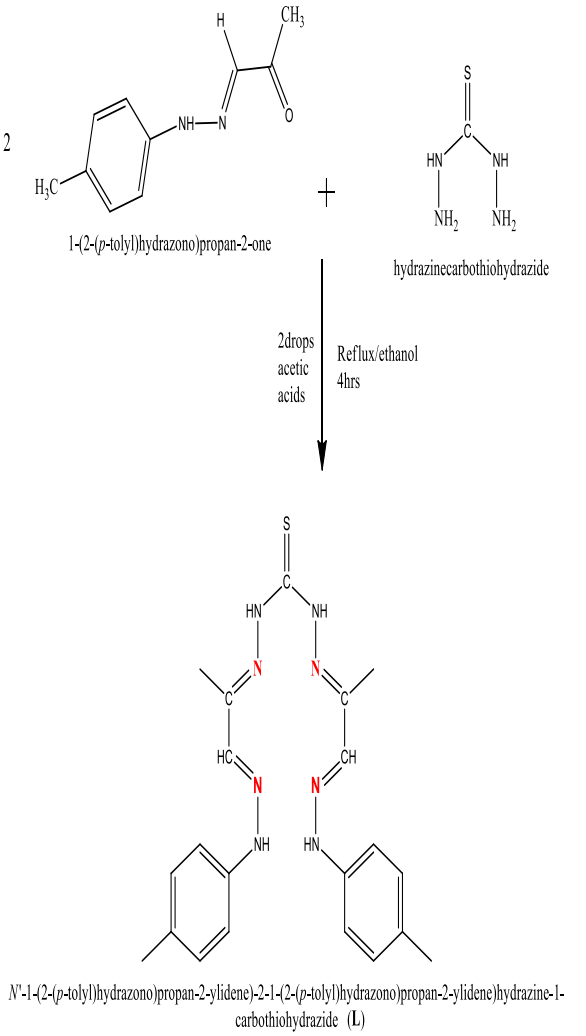

Scheme. 1: Synthesis pathway of the Schiff base ligand (L).

1.2.2. Synthesis of the metal complexes

20 ml hot ethanolic solution (70 °C) of Schiff base ligand (1 mmol, 0.442 g) was mixed with 20 ml of 1 mmole hot absolute ethanol solution of metal salts (0.266 g $CrCl_3.6H_2O$, 0.278 g $FeSO_4.7H_2O$, 0.237 g $CoCl_2.6H_2O$, 0.237 g $NiCl_2.6H_2O$, and 0.170 g $CuCl_2.2H_2O$) to synthesize the metal complexes. After 3 hours of reflux-stirring the resultant mixtures, the complexes precipitated. The precipitates were filtered off, refined by repeated washings, and dried in a vacuum over anhydrous calcium chloride. Pure metal complexes were produced via recrystallization.

1.3. Antimicrobial activity

The disc diffusion technique was used to assess the in vitro antibacterial and antifungal properties of gentamycin, ampicillin, and amphotericin B, which served as positive controls for Gram-positive and Gram-negative bacteria, respectively [14, 15]. Gram-positive bacteria (*Bacillus subtilis*, *Staphylococcus aureus*, and *Staphylococcus faecalis*), Gram-negative bacteria (*Escherichia coli*, *Pseudomonas aeruginosa*, and *Neisseria gonorrhoeae*), and a fungal strain (*Candida albicans*) were used in the study. 1 mmol stock solutions were prepared by dissolving the Schiff base ligand and its complexes in DMSO. The antibacterial activity assessment was performed using a nutrient agar medium, which was prepared, cooled to 47 °C, and seeded with microorganisms. 5 mm-diameter holes were then drilled with a sterile cork borer after the material had solidified. The examined substances were dissolved in DMSO at a concentration of 1×10^{-3} M before being added to Petri dishes (only 0.1 m). Then, fungi and bacteria were grown on these culture plates for 20 hours at 37 °C. The inhibitory zones' sizes were measured in millimeters. Evaluations of antimicrobial activity were conducted in triplicate, and the average was used as the final reading [16].

1.4. Molecular docking

The most effective drugs' potential modes of binding to the receptors of the crystal structures of *Bacillus subtilis* (3AHU), *Staphylococcus aureus* (1GHP), *Streptococcus mutans* (2ZIC), *E. coli* (1NEK), *Candida alibicans* (5JPE), and EPB in complex with tubulin in the cell cycle of cancer cells were predicted by molecular docking studies (7dae). These experiments were also conducted to determine the inhibitor's binding free energy inside the macromolecule [19,20]. They were carried out using the MOE 2008 program, an interactive molecular graphics program for calculating and showing potential docking modes of a receptor and a Schiff base ligand molecule (MOE source: Chemical Computing Group Inc., Quebec, Canada, 2008). Both the ligand and the receptor have to be provided as inputs in PDB format. The water molecules, co-crystallized ligands, and other unsupported elements (such as Na, K, and Hg) were eliminated while the amino acid chain was preserved. The Gaussian03 program was used to generate the Schiff base ligand's PDB file structure. The Protein Data Bank provided download links for the crystal structures of the various receptors (https://www.rcsb.org/).

1.5. Computational methodology

The electronic structure computations of the L and Co(II) complex were performed using the Gaussian09 suite of software [36]. For complete optimization, the DFT-based B3LYP technique and the LANL2DZ basis set were used. The TD-DFT approach and the LANL2DZ basic set were used to compute the electronic absorption spectra of the ligand and its Co(II) complex, which took into

account the influence of the solvent around the molecule. Additionally calculated was the impact of molecular orbitals on HOMO and LUMO.

Results and Discussion

Characterization of tetra dentate Schiff base ligand (L)

Orange solid Schiff base ligand (L) dissolves in typical organic solvents. All of the metal complexes and the ligand were soluble in ethanol, methanol, and DMSO but insoluble in water and stable at room temperature. The hypothesized structure was discovered to be consistent with CHNS analyses, IR spectra, and NMR data. Table 1 provides a summary of the information on the elemental analysis, color, solubility M.P., and molecular formula. The data for L's content in C, H, N, and S were found to be accurate when compared to the value estimated using the synthetic and suggested structures.

The existence of an apparent IR band at 1563 cm^{-1} caused by ν(C=N), rather than bands corresponding to ν(C=O) or ν(NH_2), confirmed the formation of the Schiff base ligand (table 2) [31]. The proton of the NH group was detected in the Schiff base ligand's ^1H NMR spectrum at 10.53 ppm, along with azomethine protons at 9.57 ppm and aromatic protons between 6.80 and 7.40 ppm (see Table 3). The synthesis of Schiff base ligand L is confirmed by the absence of any evidence for the NH_2 group.

The hypothesized formula $[C_{21}H_{26}N_8S]^{+}$ with an atomic mass of 422 amu was validated by the mass spectrum of the ligand, which showed a molecular ion peak at m/z = 422 amu matching to $[M]^+$. These investigations led to the structural resolving of the symmetric tetra-dentate Schiff base ligand.

Characterization of metal complexes

The response of ligands to metal salts was taken into consideration for the effective production of the metal complexes. Under reflux conditions, a color shift was seen when a ligand in ethanol was combined with metal(II) salts in ethanol (1:1). The estimated values and the experimental elemental analysis of complexes agreed more closely. According to Table 1, the complexes exhibit a 1:1 ML-type metal-ligand stoichiometry. The complexes have very high melting points and purity.

Table 1: Physical and analytical data of Schiff base ligand (L) and its metal complexes

Compound (chemical formula)	Color Yield (%)	M.p. (°C)	Found (Calcd)					A_m (Ω^{-1} mol^{-1} cm^2)
			C (%)	H (%)	N (%)	S (%)	M (%)	
L **($C_{21}H_{26}N_8S$)**	Orange (93)	230	59.66 (59.72)	6.07 (6.16)	26.21 (26.54)	7.17 (7.58)	-----	------
$[CrLCl_2]Cl$	Brown (89)	290	43.21 (43.39)	4.32 (4.48)	19.01 (19.28)	5.27 (5.51)	8.65 (8.95)	81
$[FeL]SO_4.2H_2O$	Brown (87)	>300	41.10 (41.31)	4.05 (4.26)	18.12 (18.36)	5.10 (5.25)	9.07 (9.18)	66
$[CoLCl_2]$	Brown (89)	300	45.29 (45.74)	4.39 (4.72)	20.09 (20.33)	5.26 (5.81)	10.13 (10.52)	26
$[NiL]Cl_2$	Brown (83)	>300	45.17 (45.65)	4.41 (4.71)	20.02 (20.29)	5.44 (5.80)	10.18 (10.68)	105
$[CuLCl_2].H_2O$	Brown(92)	200	44.21 (43.90)	4.19 (4.53)	19.16 (19.52)	5.26 (5.57)	10.14 (10.98)	23

1.5.1. IR spectral studies

Figs. 4 and 5 show infrared spectra for the main bands of the Schiff base ligand and its chelates, along with a rough assignment (Table 2). The positions of bands provide information about where ligand molecules bind when coupled to metal ions. The free ligand's IR spectra displayed three distinct bands at 3265, 1563, and 1251 cm^{-1}, which were attributed to the stretching vibrations of υ(NH), υ(C=N), and υ(C=S), respectively [32]. When comparing the spectra of the free Schiff base and its chelates, it was found that the υ(C=N) band manifested itself at a lower frequency of 1520–1552 cm^{-1} following coordination with the metal ions. The movement of electrons from nitrogen to the metal's unoccupied d-orbitals can attest to this alteration [33]. Almost identical to the free ligands, other bands maintain their places. Metal-nitrogen

bonding is confirmed by the appearance of new bands in the ranges of 44 and 409-498 cm^{-1} [34]. According to the IR data, The Schiff base ligand (L), which was previously validated by elemental analysis data, behaves as a tetra dentate ligand attaching to metal ions via four nitrogen atoms [25,33].

Table 2: Prominent infrared frequencies (4000–400 cm^{-1}) of L and its metal complexes

Compound	*υ*(NH)	*υ*(C=N)	*υ*(C=S)	*υ*(M−N)
L	3265sh	1563sh	1251sh	—
$[CrLCl_2]Cl$	3250m	1520s	1250s	4443s
$[FeL]SO_4.2H_2O$	3235sh	1522m	1248m	410s
$[CoLCl_2]$	3270sh	1550s	1250s	498w
$[NiL]Cl_2$	3235sh	1552s	1247s	409m
$[CuLCl_2].H_2O$	3270sh	1525m	1251sh	433w

sh = sharp, m = medium, s = small, w = weak and br = broad.

1.1.1. Mass spectral studies

The Schiff base ($C_{21}H_{26}N_8S$) and its complex's mass spectra revealed the molecular ion peaks shown in table 4. The mass spectra data established the metal complex's stoichiometric composition as ML. Additionally, the results of these examinations were entirely consistent with estimated molecular formulae, which are also corroborated by elemental analysis data. A strong indicator of the complexation process is the presence of the ligand moiety at 422 m/z in all complex spectra [34].

Table 3: ^{1}H NMR spectral data of the Schiff base ligand (L)

Compound	Chemical shift, (δ) ppm	Assignment
L	10.53	(s, 4H, NH)
	9.57	(s, 2H, azomethine CH)
	6.80-7.40	(m, 8H, aromatic)
	3.31	(s, 6H, CH_3)
	2.50	(s, 6H, ph-CH_3)

1.1.2. Molar conductance

The molar conductivity (Λ_m) of 10^{-3} M solutions for each complex at 25 °C could be determined because the complexes were soluble in DMF. The results showed that Cr(III), Fe(II), and Ni(II) complexes were electrolytes and ionic in nature, with molar conductance values ranging from 66 to 105 Ω^{-1} mol^{-1} cm^2. As evidence that the anion was coordinated with the metal ion, Co(II) and Cu(II) complexes showed molar conductances of 23–26 Ω^{-1} mol^{-1}. Table 1 contains a list of the data [35].

1.1.3. UV-Visible spectroscopy

The ligand and metal complexes were studied using UV-Visible spectroscopy at wavelengths between 200 and 700 nm in DMSO. The charge transfer bands π → π*, n → π* of the C=N chromophore were identified as the absorption bands at 255, 330, and 442 nm, respectively, for the Schiff base ligand. The spectra of each produced complex showed distinct changes in ligand-based transition absorption bands, indicating that the complexes were bound to the metal centers (Table 5). In the spectra of Fe(II) and Cr(III) chelate, the d-d transition was seen at 568 and 610 nm, respectively [35, 36].

Table 4: EI- mass data of L Schiff base ligand and its complexes

Compound	m/z value		Interpre-tation
	Calculated	Found	
L ($C_{21}H_{26}N_8S$)	422	422	$[M]^+$
$[CrLCl_2]Cl$	580.8	580	$[M]^+$
$[FeL]SO_4.2H_2O$	610	611	$[M+1]^+$
$[CoLCl_2]$	551	552	$[M+1]^+$
$[NiL]Cl_2$	552	552	$[M]^+$
$[CuLCl_2].H_2O$	574	574	$[M]^+$

Table 5: electronic spectral data for the ligand and its complexes

Compound	Wavelength (nm)	Type of transition
L	255, 330, 442	$\pi\rightarrow\pi^*$, $n\rightarrow\pi^*$, charge transfer
$[CrLCl_2]Cl$	234, 314, 610	$\pi\rightarrow\pi^*$, $n\rightarrow\pi^*$, d-d
$[FeL]SO_4.2H_2O$	242, 310, 568	$\pi\rightarrow\pi^*$, $n\rightarrow\pi^*$, d-d
$[CoLCl_2]$	228, 345	$\pi\rightarrow\pi^*$, $n\rightarrow\pi^*$
$[NiL]Cl_2$	287, 320	$\pi\rightarrow\pi^*$, $n\rightarrow\pi^*$
$[CuLCl_2].H_2O$	237, 359	$\pi\rightarrow\pi^*$, $n\rightarrow\pi^*$

1.5.2. Magnetic susceptibility measurements

The number of unpaired electrons and their geometric organization can be determined by measuring the magnetic susceptibility. The Cr(III) complex's magnetic moment measured 3.38 BM, confirming its octahedral geometry [33, 37]. The Co(II) complex's magnetic moment value was discovered to be 4.32 BM, indicating that it was high-spin and included three unpaired electrons in an octahedral environment. The Cu(II) complex's magnetic moments were 1.76 BM, which is compatible with the distortion of the octahedron's geometry. The Fe (II) and Ni (II) complexes have magnetic susceptibility values of (2.26 and 2.81 BM, respectively), which point to tetrahedral geometry around the metal ions [38-40].

1.5.3. Geometry optimization

Based on density functional theory (DFT), the geometries of the L Schiff base and Co(II) complex were optimized using the B3LYP functional and LANL2DZ basic set. The HOMO-LUMO energy gap (ΔE) was a crucial stability metric that was used to create theoretical explanations for the geometry, structure, and conformational barriers in numerous molecular systems [40-43]. The information about the charge transfer within the molecule has been clarified using HOMO and LUMO analysis. These calculations offer useful information about the vibrational spectrum and molecular characteristics like bond lengths and bond angles. Figs. 1 and 2 depict the frontier molecular orbital of the Schiff base ligand and Co(II) complex. The geometry of the Co(II) metal complex was shown to be better predicted by the resulting bond length and bond angle (Tables S1 & S2). As ligand L was coordinated via four nitrogen atoms, there was a modest lengthening of the bonds between N(20)-N(21), C(19)-N(20), N(16)-C(17), N(15)-N(16), N(11)-N(12), and C(10)-N(11) in the Co(II) complex. Four nitrogen atoms occupied the four equatorial places, and two chlorine atoms occupied the two axial positions. As previously mentioned, the bond angles in the Co(II) complex's coordination sphere are suggestive of a deformed octahedral geometry.

Furthermore, many relationships were used to calculate several other significant quantum parameters, including the HOMO-LUMO energy gap (ΔE), chemical potentials (*Pi*), absolute electro negativities (χ), absolute softness (σ), absolute hardness (η), global electrophilicity (ω), global softness (*S*), and additional electronic charge (ΔN *max*) as present in laterture [33, 35, 40].

The values of the estimated quantum parameters are listed in Table 6. The HOMO level was primarily focused on the nitrogen atoms in the ligand, indicating the preferred sites for the nucleophilic attack on the central metal atom [44]. The obtained results demonstrated that the $[CoLCl_2]$ complex has a narrow band gap. The increased biological activities of this metal complex are also influenced by the tiny band gap. The Co(II) complex's larger overall energy than the free ligand was a strong indication of the solid complex's stability.

Table 6: The different quantum chemical parameters of Schiff base ligand (L) and its Co(II) complex based on the DFT method

The calculated quantum chemical parameters	L	$[CoLCl_2]$
E (a.u)	**-1263.69**	**-1438.76**
Dipole moment (Debye)	**5.09**	**10.83**
E_{HOMO} (eV)	**-5.36**	**-4.89**
E_{LUMO} (eV)	**-1.93**	**-3.07**
ΔE (eV)	**3.43**	**1.82**
χ (eV)	**3.65**	**3.98**
η (eV)	**1.72**	**1.82**
σ $(eV)^{-1}$	**0.58**	**0.55**
Pi (eV)	**-3.65**	**-3.98**
S $(eV)^{-1}$	**0.29**	**0.27**
ω (eV)	**3.87**	**4.35**
ΔN_{max}	**2.12**	**2.19**

1.5.4. Molecular electrostatic potential (MEP)

Electrostatic potential V(r) maps, which are known for identifying the electronic charge distribution around the molecule surfaces and therefore predicting sites for the reactions, were calculated to examine the reactions. These maps were generated using the same optimization basis set. In the current investigation, 3D MEP plots for the ligand and its Co(II) complex were created (Figure 3).

The electron-rich region in the map, which is colored red, may typically be ordered based on the MEP (favour site for electrophilic attack). The electron-poor area, on the other hand, displays a blue color (the favourite site for nucleophilic assault) [42-44]. However, the green area denotes a region of neutral electrostatic potential.

It is clear that the L is stable because its charge density is distributed relatively uniformly. However, the negative charge surface surrounding oxygen and nitrogen atoms is higher, presumably rendering these sites more amenable to electrophilic attack (red) (Figure3). In terms of electron density, the aromatic ring appears neutral.

Thus, the potential distribution favours the complexation reaction [45], which is further supported by the electrostatic potential distribution of the Co(II) complex, in which the metal core is surrounded by a stronger negative charge (Figure 3b). Nitrogen atoms in the Co(II) complex have higher electronegativity than free L, making them the preferred target of an electrophilic attack by a metal ion.

1.6. Biological activity

The in vitro antibacterial and antifungal properties of each of the newly synthesized compounds were examined. The average diameter of the zones that each tested drug inhibited bacterial growth in around the well, measured in millimeters, was the result.

The outcomes are displayed in Figure 4 and Table 7. Compared to the free ligand, each metal complex has greater bactericide and fungicide potency (L). The data also show that, although the degree of a given compound's action within the same type of bacterium varies, complexes are somewhat more efficient against Gram-positive strains than they are against Gram-negative

ones. This difference in activity may be explained by the fact that Gram-positive bacteria's cell walls have greater antigenic qualities since their outer lipid membranes are composed of polysaccharides. Even though the complexes had promising antibacterial activity against the bacterial strains, it was discovered that these activities were comparable to those of ordinary ampicillin (antibacterial drug).

The effective diffusion of the metal complexes into the bacterial cells or contact with the bacterial cell walls was hypothesized to be responsible for this increase in activity. According to the findings, Co(II) complex displayed the strongest antibacterial and antifungal properties. There are additional criteria for antibacterial action besides chelation.

The antimicrobial activity is greatly influenced by many significant parameters, including the nature of the metal ion, the nature of the ligand, coordinating sites, and geometry of the complex, concentration, hydrophobicity, lipophilicity, and the presence of co-ligands.

The hazardous substance cannot penetrate the bacterial cell wall if the geometry and charge distribution around the molecule is incompatible with the geometry and charge distribution surrounding the pores of the bacterial cell wall.

This prevents the toxic reaction from occurring inside the pores. This might help to explain why some complexes have weak activity [40-45].

TABEL 7. Biological activity of L ligand and its metal complexes

Sample		Inhibition zone diameter (mm / mg sample)						
		Gram-positive bacterial species			Gram-negative bacterial species			Fungi
		Bacillus subtilis	*Staphylococcus aureus*	*Staphylococcus faecalis*	*E.coli*	*Neisseria gonorrhoeae*	*Pseudomonas aeruginosa*	*Candida alibicans*
L		10	9	9	10	9	9	NA
$[CrLCl_2]Cl$		16	14	14	16	14	14	NA
$[FeL]SO_4.2H_2O$		12	12	14	13	12	13	NA
$[CoLCl_2]$		22	24	22	22	20	20	15
$[NiL]Cl_2$		10	11	13	10	14	14	9
$[CuLCl_2].H_2O$		18	15	14	17	15	15	13
Standard	Ampicillin	26	26	21	25	28	26	-----
	Amphotericin B	-----	-----	-----	-----	-----	-----	21

NA: no activity Ampicillin: Standard antibacterial agent; Amphotericin B: Standard antifungal agent.

1.7. Molecular docking investigation

Drug development is frequently carried out computationally using molecular docking [76]. Modeling the mechanism of molecular recognition is the focus of molecular docking. With the best comparative orientation between them, the best protein (receptor) and drug combination are sought after through molecular docking to reduce the free energy of the entire system.

To better understand how different proteins representing various types of bacterial and fungal species interact with the Schiff base ligand (L) and its Co(II) complex, a MOE-docking simulation was conducted. In addition, the PDB co-crystal form of the protein 7dea from cancer cells was used for this simulation due to its function in cancer cell proliferation.

An overview of their drug-like efficacy is provided by pharmacokinetics, and the two compounds showed strong interactions with a variety of receptors, particularly the fungal 5jPE receptor. The patterns will be provided via MOE docking (Fig. 5) [43,45].

Using interaction patterns as a guide, it was determined that distinct docking scores with the L and Co(II)-L complexes vs 5jpe were obtained (-4.6 and -9.6 kcal/mol, respectively). H-bonding interaction is the primary method by which the L and Co(II)-L complex binds to protein receptors.

Because L and Co(II)-L combination effectively bind with proteins and inhibit active sites in the biological system, their cytotoxicity was predicted.

They can think of prospective cancer treatments based on how the L and Co(II)-L combination interacts with the protein 7dea found on cancer cells.

Conclusion

In this study, the tetra dentate Schiff base ligand and its transition metal (II)/(III) complexes are studied using magnetic investigations, mass spectroscopy, IR, UV-visible, and UV-visible spectroscopy. The outcomes of these investigations led to coordination compounds containing tetrahedral-shaped Ni(II) and Fe(II) complexes and octahedral-shaped Cr(II), Co(II), and Cu(II) complexes. Similar to how the electron-donating potentials of the complexes have a substantial impact on biological activities, the HOMO-LUMO energies in DFT investigations showed modest alterations due to electron charge density distribution, which affected their biological capabilities. The results of the molecular docking experiments showed that the compounds' interactions and binding energies with numerous bacterial, fungal, and cancer cell proteins were favourable. This suggests that the drugs need more effective bio targets.

Conflicts of interest

There are no conflicts to declare.

Formatting of funding sources

No fuding source is present

References

1. Mohapatra, R. K., Sarangi, A. K., Azam, M., El-ajaily, M. M., Kudrat-E-Zahan, M., Patjoshi, S. B., & Dash, D. C. (2019). Synthesis, structural investigations, DFT, molecular docking and antifungal studies of transition metal complexes with benzothiazole based Schiff base ligands. Journal of Molecular Structure, 1179, 65–75.
2. Aboelmagd, A., Ali, I. A. I., Salem, E. M. S., & Abdel-Razik, M. (2013). Synthesis and antifungal activity of some s-mercaptotriazolobenzothiazolyl amino acid derivatives. European Journal of Medicinal Chemistry, 60, 503–511.
3. Pejchal, V., Pejchalová, M., & Růžičková, Z. (2015). Synthesis, structural characterization, antimicrobial and antifungal activity of substituted 6-fluorobenzo [d] thiazole amides. Medicinal Chemistry Research, 24(10), 3660–3670.
4. Racane, L., Tralic-Kulenovic, V., & Fiser-Jakic, L. (2001). Synthesis of bis-substituted amidinobenzothiazoles as potential anti-HIV agents. Heterocycles, 55(11), 2085–2098.
5. Patel, N. B., Purohit, A. C., & Rajani, D. (2014). Newer thiazolopyrimidine-based sulfonamides clubbed with benzothiazole moiety: synthesis and biological evaluation. Medicinal Chemistry Research, 23(11), 4789–4802.
6. Lu, F., Hu, R., Wang, S., Guo, X., & Yang, G. (2017). Luminescent properties of benzothiazole derivatives and their application in white light emission. RSC Advances, 7(7), 4196–4202.
7. Piscitelli, F., Ballatore, C., & Smith III, A. B. (2010). Solid phase synthesis of 2-aminobenzothiazoles. Bioorganic & Medicinal Chemistry Letters, 20(2), 644–648.
8. Dash, D. C., Mahapatra, A., Mohapatra, R. K., Ghosh, S., & Naik, P. (2008). Synthesis and characterization of UÜ2 (VI), Th (IV), ZrO (IV) and VO (IV) complexes with 1, 11-dihydroxy-1, 4, 5, 7, 8, 11-hexaaza-2, 3, 9, 10-tetramethyl-1, 3, 8, 10-decatetraene-6-thione and their derivatives with choloacetic acid. Indian J. Chem., 47, 1009–1013.
9. Mohapatra, R. K., & Dash, D. C. (2010). Synthesis and Characterization of UO 2 (VI), Th (IV), ZrO (IV) and VO (IV) Complexes with Schiff-Base Octaazamacrocyclic Ligands. Journal of the Korean Chemical Society, 54(4), 395–401.
10. Mondal, S., Mandal, S. M., Mondal, T. K., & Sinha, C. (2017). Spectroscopic characterization, antimicrobial activity, DFT computation and docking studies of sulfonamide Schiff bases. Journal of Molecular Structure, 1127, 557–567.
11. Ayoub, M. A., Abd-Elnasser, E. H., Ahmed, M. A., & Rizk, M. G. (2018). Some new metal (II) complexes based on bis-Schiff base ligand derived from 2-acetylethiophine and 2, 6-diaminopyridine: Syntheses, structural investigation, thermal, fluorescence and catalytic activity studies. Journal of Molecular Structure, 1163, 379–387.
12. Turan, N. (2019). Synthesis, spectroscopy, optical characteristics and parameters of Co (II), Pd (II) complexes and Schiff base ligand. Journal of Electronic Materials, 48(11), 7366–7371.
13. Zaltariov, M., Vieru, V., Zalibera, M., Cazacu, M., Martins, N. M. R., Martins, L. M., Rapta, P., Novitchi, G., Shova, S., & Pombeiro, A. J. L. (2017). A Bis (μ-chlorido)-Bridged Cobalt (II) Complex with Silyl-Containing Schiff Base as a Catalyst Precursor in the Solvent-Free Oxidation of Cyclohexane. European Journal of Inorganic Chemistry, 2017(37), 4324–4332.
14. Cozzi, P. G. (2004). Metal–Salen Schiff base complexes in catalysis: practical aspects. Chemical Society Reviews, 33(7), 410–421.
15. Maity, T., Saha, D., Bhunia, S., Brandao, P., Das, S., & Koner, S. (2015). A family of ligand and anion dependent structurally diverse Cu (II) Schiff-base complexes and their catalytic efficacy in an O-arylation reaction in ethanolic media. RSC Advances, 5(100), 82179–82191.
16. Parsaei, M., Asadi, Z., & Khodadoust, S. (2015). A sensitive electrochemical sensor for rapid and selective determination of nitrite ion in water samples using modified carbon paste electrode with a newly synthesized cobalt (II)-Schiff base complex and magnetite nanospheres. Sensors and Actuators B: Chemical, 220, 1131–1138.
17. A.A. El-Sherif, M.M. Shoukry, L.O Abobakr, Spectrochimica Acta - Part A: Molecular and Biomolecular Spectroscopy, 112(2013) 290-300.
18. Wang, S., Yang, X., Zhu, T., Bo, L., Wang, R., Huang, S., Wang, C., Jiang, D., Chen, H., & Jones, R. A. (2018). Construction of luminescent high-nuclearity Zn–Ln rectangular nanoclusters with flexible long-chain Schiff base ligands. Dalton Transactions, 47(1), 53–57.
19. Wang, Y., Mao, P.-D., Wu, W.-N., Mao, X.-J., Fan, Y.-C., Zhao, X.-L., Xu, Z.-Q., & Xu, Z.-H. (2018). New pyrrole-based single-molecule multianalyte sensor for Cu2+, Zn2+, and Hg2+ and its AIE activity. Sensors and Actuators B: Chemical, 255, 3085–3092.

20. Kumar, A., Lionetti, D., Day, V. W., & Blakemore, J. D. (2018). Trivalent Lewis acidic cations govern the electronic properties and stability of heterobimetallic complexes of nickel. Chemistry–A European Journal, 24(1), 141–149.
21. Zhang, J., Xu, L., & Wong, W.-Y. (2018). Energy materials based on metal Schiff base complexes. Coordination Chemistry Reviews, 355, 180–198.
22. Singh, V. K., Kadu, R., Roy, H., Raghavaiah, P., & Mobin, S. M. (2016). Phenolate based metallomacrocyclic xanthate complexes of Co II/Cu II and their exclusive deployment in [2: 2] binuclear N, O-Schiff base macrocycle formation and in vitro anticancer studies. Dalton Transactions, 45(4), 1443–1454.
23. Naik, K. H. K., Selvaraj, S., & Naik, N. (2014). Metal complexes of ONO donor Schiff base ligand as a new class of bioactive compounds; synthesis, characterization and biological evolution. Spectrochimica Acta Part A: Molecular and Biomolecular Spectroscopy, 131, 599–605.
24. Kaya, İ., Daban, S., & Şenol, D. (2021). Synthesis and characterization of Schiff base, Co (II) and Cu (II) metal complexes and poly (phenoxy-imine) s containing pyridine unit. Inorganica Chimica Acta, 515, 120040.
25. Sudha, A. (2022). Investigation of new schiff base transition metal (II) complexes theoretical, antidiabetic and molecular docking studies. Journal of Molecular Structure, 1259, 132700.
26. Refat, M. S., Saad, H. A., Gobouri, A. A., Alsawat, M., Adam, A. M. A., & El-Megharbel, S. M. (2022). Charge transfer complexation between some transition metal ions with azo Schiff base donor as a smart precursor for synthesis of nano oxides: An adsorption efficiency for treatment of Congo red dye in wastewater. Journal of Molecular Liquids, 345, 117140.
27. A.A. El-Sherif, A. Fetoh , Yasir Kh. Abdulhamed , G. M. Abu El-Reash, Inorg Chim. Acta 480 (2018) 1–15.
28. G.A.M Elhagali, G.A Elsayed, R.A. Eliswey, A.A. El-Sherif, J of the Iranian Chemical Society,15(6) (2018) 1243-1254.
29. A. I. Vogel, Quantitative Inorganic Analysis Including Elemental Instrumental Analysis, 2nd ed., Longmans, London, 1962.
30. A.T. Abdelkarim, W.H. Mahmoud, A.A. El-Sherif, Journal of Molecular Liquids, 328 (2021) , 115334.
31. Abd El-Wahab, H., Abd El-Fattah, M., El-Alfy, H. M. Z., Owda, M. E., Lin, L., & Hamdy, I. (2020). Synthesis and characterisation of sulphonamide (Schiff base) ligand and its copper metal complex and their efficiency in polyurethane varnish as flame retardant and antimicrobial surface coating additives. Progress in Organic Coatings, 142, 105577.
32. Palanimurugan, A., & Kulandaisamy, A. (2018). DNA, in vitro antimicrobial/anticancer activities and biocidal based statistical analysis of Schiff base metal complexes derived from salicylalidene-4-imino-2, 3-dimethyl-1-phenyl-3-pyrazolin-5-one and 2-aminothiazole. Journal of Organometallic Chemistry, 861, 263–274.
33. A.A. El-Sherif, A.A El-Sisi, M. Ali, O. AlTaweel, A.T AbdEl-Karim, International Journal of Electrochemical Science, 15(11)(2020) 10885-10907.
34. Abd El-Razek, S. E., El-Gamasy, S. M., Hassan, M., Abdel-Aziz, M. S., & Nasr, S. M. (2020). Transition metal complexes of a multidentate Schiff base ligand containing guanidine moiety: Synthesis, characterization, anti-cancer effect, and anti-microbial activity. Journal of Molecular Structure, 1203, 127381.
35. Emad S. Mousa, Walaa H. Mahmoud, Appl Organometal Chem. 33:e4844 (2019) 1-18.
36. De, A., Ray, H. P., Jain, P., Kaur, H., & Singh, N. (2020). Synthesis, characterization, molecular docking and DNA cleavage study of transition metal complexes of o-vanillin and glycine derived Schiff base ligand. Journal of Molecular Structure, 1199, 126901.
37. Sathyanarayana, D. N. (2001). Electronic absorption spectroscopy and related techniques. Universities Press.
38. Ghosh, A. K., Mitra, M., Fathima, A., Yadav, H., Choudhury, A. R., Nair, B. U., & Ghosh, R. (2016). Antibacterial and catecholase activities of Co (III) and Ni (II) Schiff base complexes. Polyhedron, 107, 1–8.
39. Tofiq, D. I., Hassan, H. Q., & Abdalkarim, K. A. (2021). Preparation of a novel Mixed-Ligand divalent metal complexes from solvent free Synthesized Schiff base derived from 2, 6-Diaminopyridine with cinnamaldehyde and 2, 2′-Bipyridine: Characterization and antibacterial activities. Arabian Journal of Chemistry, 14(12), 103429.
40. Osowole, A. A. (2008). Syntheses and characterization of some tetradentate Schiff-base complexes and their heteroleptic analogues. E-Journal of Chemistry, 5(1), 130–135.
41. Osowole, A. A., Kolawole, G. A., & Fagade, O. E. (2008). Synthesis, characterization and biological studies on unsymmetrical Schiff-base complexes of nickel (II), copper (II) and zinc (II)

and adducts with 2, 2′-dipyridine and 1, 10-phenanthroline. Journal of Coordination Chemistry, 61(7), 1046–1055.

42. Bansod, A., Bhaskar, R., Ladole, C., Salunkhe, N., Thakare, K., & Aswar, A. (2022). Synthesis, Characterization, Biological Activity and Solid-State Electrical Conductivity Study of Some Metal Complexes Involving Pyrazine-2-Carbohydrazone of 2-Hydroxyacetophenone. Journal of Transition Metal Complexes, 5.
43. Manjuraj, T., Yuvaraj, T. C. M., Jayanna, N. D., & Sarvajith, M. S. (2022). Design, spectral, thermal, DFT studies, antioxidant and molecular docking studies of pyrazole-based schiff base ligand and its metal (II) complexes. Materials Today: Proceedings, 54, 646–655.
44. El-Gammal, O. A., El-Bindary, A. A., Mohamed, F. S., Rezk, G. N., & El-Bindary, M. A. (2022). Synthesis, characterization, design, molecular docking, anti COVID-19 activity, DFT calculations of novel Schiff base with some transition metal complexes. Journal of Molecular Liquids, 346, 117850.
45. Alharbi, A., Alzahrani, S., Alkhatib, F., Al-Ola, K. A., Alfi, A. A., Zaky, R., & El-Metwaly, N. M. (2021). Studies on new Schiff base complexes synthesized from d10 metal ions: Spectral, conductometric measurements, DFT and docking simulation. Journal of Molecular Liquids, 334, 116148.